

Headcut Erosion in Wyoming's Sweetwater Subbasin

Samuel E. Cox¹ · D. Terrance Booth² · John C. Likins³

Received: 28 October 2014 / Accepted: 10 September 2015 / Published online: 26 September 2015
© Springer Science+Business Media New York (outside the USA) 2015

Abstract Increasing human population and intensive land use combined with a warming climate and chronically diminished snowpacks are putting more strain on water resources in the western United States. Properly functioning riparian systems slow runoff and store water, thus regulating extreme flows; however, riparian areas across the west are in a degraded condition with a majority of riparian systems not in proper functioning condition, and with widespread catastrophic erosion of water-storing peat and organic soils. Headcuts are the leading edge of catastrophic channel erosion. We used aerial imagery (1.4–3.3-cm pixel) to locate 163 headcuts in riparian areas in the Sweetwater subbasin of central Wyoming. We found 1-m—the generally available standard resolution for land management—and 30-cm pixel imagery to be inadequate for headcut identification. We also used Structure-from-Motion models built from ground-acquired imagery to model 18 headcuts from which we measured soil loss of 425–720 m³. Normalized by channel length, this represents a loss of 1.1–1.8 m³ m⁻¹ channel. Monitoring headcuts, either from ground or aerial imagery, provides an objective indicator of sustainable riparian land management and

identifies priority disturbance-mitigation areas. Image-based headcut monitoring must use data on the order of 3.3 cm ground sample distance, or greater resolution, to effectively capture the information needed for accurate assessments of riparian conditions.

Keywords Riparian · Wetland · Monitoring · Structure-from-motion · Remote sensing

Introduction

The world's functional meadows and wetlands spread, store, and regulate water flow (Heede 1978; Naiman and Décamps 1997); conserve soil and support plant productivity (Avni 2005); store carbon (Chimner and Cooper 2003; Miller and Fujii 2010), filter nutrients and particulates; and provide for biological diversity (Naiman and Décamps 1997; Zald 2009). Riparian ecosystems of the US West cover only 1 % of the area, yet support a majority of the plants and animals (Kauffman et al. 1997; USGAO 1988; Belsky et al. 1999). However, headcut erosion in these systems has resulted in significant losses of riparian soil–water–carbon reservoirs and derivative ecological services (Stavi et al. 2010).

Headcuts are the most dynamic feature of gully erosion, the principal channel erosion point, and the principal source of eroded sediment (Martinez-Casasnovas et al. 2004). Between 1990 and 2001, Avni (2005) measured total gully-erosion soil loss of 800–9000 m³ at three sites in the Negev Highlands (Israel) that destroyed meadows and reduced vegetative production 70–90 % with "...rich herbaceous vegetation..." above headcuts and "...almost negligible..." herbaceous vegetation below headcuts. Such ecological-state transitions also affect soil organic matter

Electronic supplementary material The online version of this article (doi:[10.1007/s00267-015-0610-1](https://doi.org/10.1007/s00267-015-0610-1)) contains supplementary material, which is available to authorized users.

✉ Samuel E. Cox
secox@blm.gov

¹ USDI Bureau of Land Management, 5353 Yellowstone Rd, Cheyenne, WY 82009, USA

² USDA Agricultural Research Service, 8408 Hildreth Rd, Cheyenne, WY 82009, USA

³ USDI Bureau of Land Management, 1335 Main St, Lander, WY 82520, USA

(SOM) and water storage. Since all soil-texture groups increase in available water-holding capacity as organic matter content increases (Hudson 1994; Bigelow et al. 2004; Nusier 2004), lost SOM represents lost water-storage capacity in systems that should hold water like a sponge and gradually release it downstream (Forsling 1931; US-GAO 1988). Similarly, SOM holds nutrients that are lost when SOM is lost (Zheng et al. 2005). Intact riparian systems filter water, reducing sediment load to effect cleaner downstream water, but damaged systems contribute sediment. Poesen et al. (2003) reported that sediment yield was 13× higher in catchments with numerous eroding gullies compared to catchments with no eroded gullies. The same authors reviewed 56 gully-erosion studies and reported that gully-erosion soil loss accounts for 10–94 % of total sediment yield from water erosion, a wide interval attributed to differences in temporal and spatial scales of the studies. Osborn and Simanton (1986) reported that a single headcut contributed 25 % of a suspended sediment load, and Hunsaker and Neary (2012) calculated that headcut erosion contributed 4× more sediment load than bank erosion. Meadow and wetland destruction by gully erosion is most common in hot deserts of temperate climates (Avni 2005) but also occurs in cold deserts and other temperate-climate biomes particularly after fire, overgrazing (Heede 1978), or other disturbance has upset channel stability.

Headcuts occur when alluvial deposition within a channel exceeds a slope that can withstand peak runoff events (Schumm and Hadley 1957). This “critical angle” of slope is determined by the alluvial substrate and vegetative cover, both within the channel and the catchment area. Catchment area is correlated with headcut retreat, as a larger catchment sends more water through a channel during peak runoff (Vandekerckhove et al. 2003). Yet catchment effects are highly influenced by vegetative cover (Bull 1997; Vandekerckhove et al. 2000), and ample evidence shows that poor grazing management degrades vegetative cover on upland rangelands and causes increased runoff (Forsling 1931; Brown and Schuster 1969; Lusby 1970; Meeuwig 1970; Stoddart et al. 1975; McCalla et al. 1984; Greene et al. 1994). Climate also plays a role (Bull 1997), and recent higher mean annual temperatures in the western US (Barnett et al. 2008; Parolo and Rossi 2008; Pauchard et al. 2009; Pepin and Lundquist 2008; Nayak et al. 2010; Mealor et al. 2012) could serve to exacerbate erosion by shifting precipitation from snow to rain, an effect already documented along the west coast (Knowles et al. 2006; BOR 2013), with rain driving more channel erosion than snowmelt (Forsling 1931). The common threat of all factors outside of soil chemistry, including roads, trails, cultivation, logging, grazing, and—over the long term—climate change, is the degradation of natural

vegetation (Bull 1997, Poesen et al. 2003, Stavi et al. 2010). This is further substantiated by Antevs (1952) who argued that headcutting in arroyos of the southwestern US since 1880 was principally caused by degraded plant cover from improper livestock grazing. Trimble and Mendel (1995) and Bull (1997) commented on water-table lowering by channel entrenchment as leading to decreased vegetation and converting plant communities from riparian to upland types (Castelli et al. 2000, Stromberg 2001, Dwire et al. 2006), a transition that increases runoff and erosion force and further incises the channel. Over time, this channel erosion and falling water table reduce habitat quality for riparian obligates by disconnecting the channel from the floodplain, often converting perennial streams to intermittent flows (Beschta et al. 2012).

Over the last 15 years, Wyoming experienced both damaging spring floods and costly summer droughts. Consequences of these events could be ameliorated with regulated water flow provided by properly functioning riparian reaches. Given current and projected reductions in snowpack, and earlier spring snowmelt, western US river late-season flows may become increasingly unreliable (Mote et al. 2005, Regonda et al. 2005, Barnett et al. 2008, EPA 2014, Nijhuis 2014), increasing the need for water storage. Natural, dispersed water storage provided by functional riparian systems reduces the need for downstream reservoirs and the associated ecological, geomorphological, social, and economic complications of siting and constructing dams (e.g., Turner and Karpiscak 1980, Ligon et al. 1995, Tilt et al. 2009). These are all good reasons why the very first page of the Bureau of Land Management’s 2002 allotment evaluation for much of the public land in the Sweetwater subbasin establishes that a key management goal is to “restore or maintain shallow ground water tables in association with riparian areas...” (BLM 2002). This goal is literally undercut by headcut erosion. Monitoring headcuts is thus essential, and especially so in light of recent changes in grazing plans mandated by court ruling (USDI 2014), and due to anticipated climate and hydrologic trends. Here, we discuss the extent and implication of gully erosion in the Sweetwater subbasin and the remote sensing techniques capable of facilitating effective riparian monitoring.

Because of the high cost of ground-based riparian monitoring in the vast Sweetwater River subbasin, Wyoming, USA, US Department of the Interior, Bureau of Land Management (BLM) surveys of resource conditions in that area have been infrequent and at low sample densities (BLM 2002). To address this data deficiency, BLM contracted, in 2008, for an aerial survey capturing nested very large-scale aerial (VLSA) images at 0.2, 1.4, and 3.3 cm ground sample distance (GSD) along ~150 km of ephemeral and perennial streams.

Our question was whether the 0.2–3.3-cm GSD of the 2008 imagery provided information not available from standard 1-m imagery and, if so, whether that information could be used to enhance riparian ground-monitoring efforts. We used the 2008 imagery and public-domain 1-m GSD National Agriculture Imagery Program (NAIP) imagery to inventory headcuts and other erosion features. We then intensively sampled selected features on the ground to create 3-dimensional models facilitating fine-scale soil loss measurements and to provide baseline positions for determination of gully erosion rate, both from headcuts and from sidewall sloughing in incised channels. Our approach served to both locate headcuts and measure their dimensions in fine detail.

Methods

Site Description

The semiarid cold desert in the upper portion of the Sweetwater subbasin (HUC 8-10180006, USGS 2014a) is largely treeless rangeland of rolling hills crossed by wet meadows and spring-fed streams, with uplands dominated by sagebrush (*Artemisia tridentata* Nutt. ssp. *wyomingensis* Beetle and Young; *Artemisia tridentata* Nutt. ssp. *vaseyanus* (Rydb.) Beetle) and perennial grasses (*Pseudoroegneria spicata* (Pursh) Á. Löve; *Pascopyrum smithii* (Rydb.) Á. Löve; *Koeleria macrantha* (Ledeb.) Schult; *Hesperostipa comata* (Trin. & Rupr.) Barkworth). Riparian areas comprise <1 % of the area and are dominated by Nebraska sedge (*Carex nebrascensis* Dewey).

Most of the 125,000-ha study area (-108.4° , 42.4° ; 2200 m mean elevation; Fig. 1) is managed by the BLM. Annual precipitation is 30–40 cm, mostly as snow. Livestock grazing began here in the 1840s and continues today under BLM management as several public grazing allotments formerly comprising the Green Mountain Common Allotment (GMCA). The historic livestock (sheep and cattle) season of use has been 10 May to 10 November (185 days). Livestock actual use from 1980 to 2010 was 22,923 animal unit months (AUMs) or 8.2 ha AUM^{-1} , averaging 48 % of the permitted 47,361 AUMs or 4.0 ha AUM^{-1} (USDI 2014). In semiarid rangelands, livestock spend disproportionate time in riparian areas where moisture produces more abundant forage than surrounding uplands (Kauffman and Kreuger 1984). Consequently, riparian areas in the study area show more effects of 150 years of livestock grazing than do surrounding uplands (Corning 2002). In 2002, only 14 % of lotic habitat and 26 % of lentic habitat in the GMCA were in proper functioning condition or on an upward trend (BLM 2002). All of these conclusions were based on only 8 upland and 18

riparian transects regularly monitored within the half-million-acre GMCA (BLM 2002). Such sparse sampling leaves analysis particularly vulnerable to a Type II statistical error—a false negative—due to inadequate statistical power (Mudge et al. 2012). To more accurately describe the area, a landscape-level sampling approach is needed that incorporates more sampling. Additional metrics such as surface roughness (Booth et al. 2014) and headcut size and retreat rate would provide managers with more evidence to determine habitat quality trends.

Headcut Identification from Aerial Imagery

Remote sensing is one method to accomplish landscape-level assessments. Intermittent color (red, green, blue) aerial images were captured in June 2008 along ~ 150 km of ephemeral and perennial streams (Fig. 1), and used to locate erosion features in riparian areas. The survey was conducted from a light sport airplane (FAA 2010) flying at mean altitude above ground level of 188 m. The pilot manually triggered cameras, assisted by GPS navigation. Nested, nadir images were simultaneously acquired at each sample location using (1) a navigation system, (2) three digital cameras (Table 1), (3) a laser altimeter, and (4) a laptop running Snapshot navigation software (Track'Air, Oldenzaal, Netherlands; Booth and Cox 2006). These images do not provide continuous riparian area coverage, but are discrete samples at 100–200-m intervals. Primarily, 1.4-cm GSD images were used to locate erosion features. Other resolutions were used occasionally to confirm detail (0.2 cm) or context (3.3 cm). Because the 2008 imagery was acquired intermittently, we used NAIP 1-m GSD natural color orthoimagery, acquired in 2012, to locate erosion features potentially not located within the 1.4-cm GSD images. NAIP imagery is the standard, public-access image product used by public land management agencies like the BLM for all manner of resource monitoring. Locations of headcuts identified from 1.4-cm GSD imagery were recorded in a GIS (Fig. 1), and eight were visited in October 2011 for ground observation. During this field visit, additional headcut locations were recorded and selections made for further study.

Terrain Model Creation and Volumetric Soil Loss Assessment from Ground-Based Imagery

Structure-from-motion (SfM) is the process of recreating an object's structure from multiple images acquired from a moving sensor (Westoby et al. 2012). Nineteen distinct, ground-observed headcuts distributed among 14 drainages were selected for SfM modeling to calculate headcut spatial and volumetric extent (Table 2).

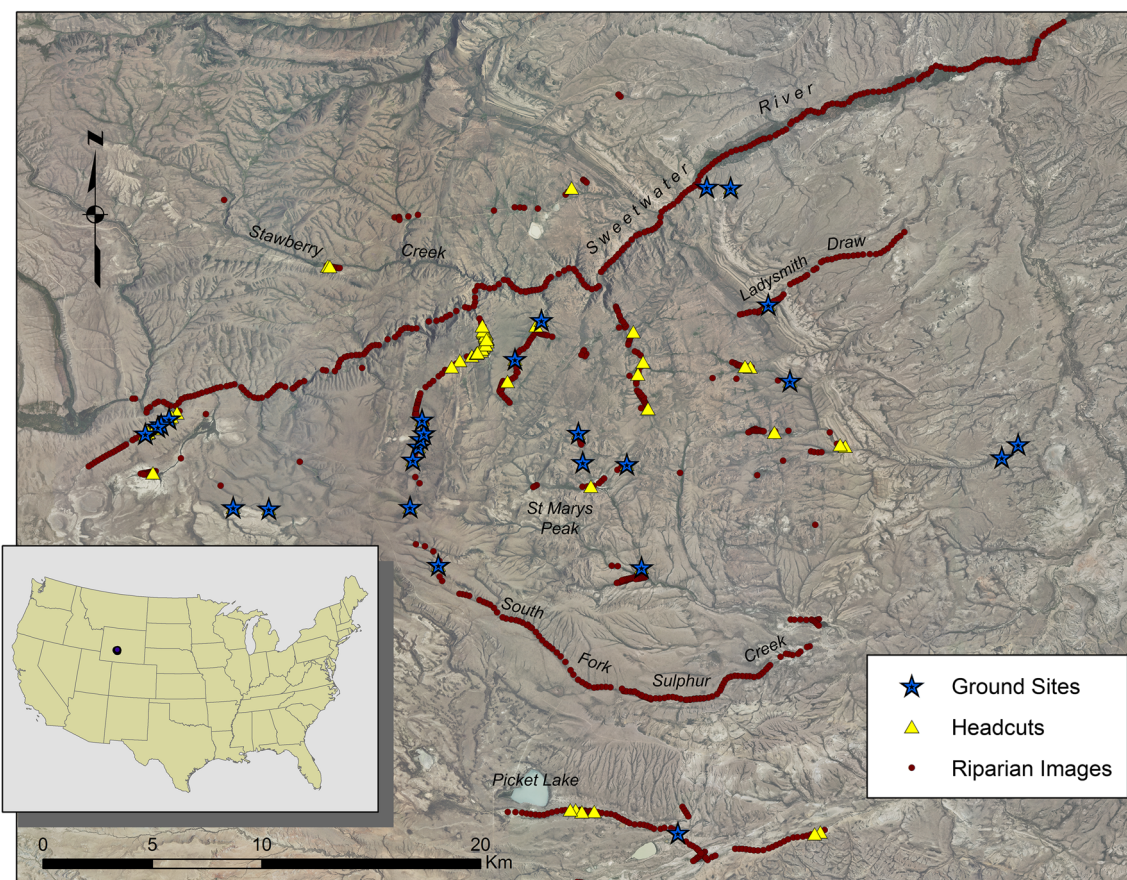


Fig. 1 Central Wyoming study area showing (1) twenty-six ground measurement sites, (2) seventy-three sites with headcuts identified from 1.4-cm GSD aerial imagery, and (3) all 1.4-cm GSD aerial images capturing riparian areas or river channels (color online)

Table 1 Three cameras captured nested, nadir images at each imaged location. Nominal ground sample distance (GSD), field of view (FOV), and image area are based on the mean aircraft altitude above ground level of 188 m for the 1099 riparian locations

Camera	Sensor	Lens (mm)	GSD (cm)	FOV X (m)	FOV Y (m)	Area (m ²)
Canon 1Ds	11 MP	50	3.3	134.6	89.5	12,045
Canon 1Ds Mk II	16.7 MP	100	1.4	67.7	45.1	3,053
Canon 1Ds Mk II	16.7 MP	840 ^a	0.2	8.1	5.4	43

^a 600-mm lens with 1.4× teleconverter

Ground control points (GCPs) were created using five white, numbered 12-cm digital video disks (DVDs) anchored to the ground with a nail at equidistant points around and in the headcut and downstream scour, encompassing an area ~1 m upstream and ≤50 m downstream of the knickpoint (depending on scour length below the headcut), and including ~1 m on either side of the eroded area. GCPs encompassed the full range of elevation in the sampled area. We used a Trimble GeoXH and Zephyr antenna (Trimble, Sunnyvale, CA) on a 2-m tripod to collect coordinates for 2 min disk⁻¹, and post-processed the data with Pathfinder Office v5.3 (Trimble).

Following guidelines for close-range photogrammetry suggested by Mathews (2008), we used a D800 36-megapixel camera with a 28-mm lens (Nikon Corp., Tokyo, Japan) in aperture priority mode to capture color (red, green, blue) digital images (7360×4912 pixels) with minimal JPG compression. The lens was focused manually and taped for constant lens position at each site, which is critical for maintaining a constant lens element orientation for calibration (Mathews 2008). Images were acquired by holding the camera at eye level and shooting toward the center of the channel while circling clockwise around the feature in short intervals to achieve 70–80 % image

Table 2 Site analysis, including the number of images used to create the surface model, the model root mean square error (RMSE), and measured relative spatial error, and the estimated range of soil loss due to headcut erosion from each site, both for the total headcut and

scour area, and normalized by the thalweg distance in the model. See online supplementary materials for terrain models and coordinates for all sites

Site	Drainage	Images used in model	Model RMSE (pixels)	Model Error (mm)	Soil loss	
					$\text{m}^3 \text{ headcut}^{-1}$	$\text{m}^3 \text{ m channel}^{-1}$
665	N Fork Sulphur Creek	316	0.34	0.2	43.8–131.5	0.81–2.43
998	Harris Slough	180	0.34	0.8	1.1–4.6	0.07–0.29
1336	Coyote Gulch	176	0.34	0.9	1.8–2.1	0.18–0.20
1494	Sweetwater River	138	0.44	0.3	26.7–36.5	2.26–3.09
1557	Ladysmith Draw	254	0.37	1.0	na ^a	na
1700	Wagon Tire Spring	171	0.33	0.4	12.6–13.1	1.03–1.07
1747	Wagon Tire Spring	159	0.33	1.0	2.3–6.4	0.20–0.57
1979	Long Slough	165	0.99	7.0	3.5–5.9	0.46–0.78
1982	Long Slough	209	0.36	2.0	3.9–4.4	0.49–0.55
1987	Long Slough	147	0.41	2.0	3.5–6.2	0.69–1.22
2211	Picket Creek	297	0.33	3.0	6.7–16.6	0.15–0.38
2500	Granite Creek	231	0.53	0.2	16.4–33.2	0.75–1.52
2502	Granite Creek	203	0.82	5.0	40.9–45.8	1.92–2.14
2504	Granite Creek	162	0.73	1.0	4.3–4.4	0.44–0.45
2536	Mormon Creek	285	0.34	0.3	31.0–36.2	1.83–2.13
2551	Mormon Creek	242	0.30	0.5	9.4–11.4	0.62–0.75
2741	S Fork Sulphur Creek	287	0.34	0.4	34.8–42.0	1.84–2.22
L Coyote	Coyote Gulch	415	0.79	9.0	133.2–191.3	4.90–7.03
M Coyote	Coyote Gulch	508	0.49	9.0	49.6–128.5	1.88–4.89
Mean		239	0.47	2.3	23.6–40.0	1.1–1.8

^a Headcut was not well defined; no volume measurements were made

overlap, with camera distance, height, and rotation varied during multiple passes in an attempt to capture every surface in at least three images from varying perspectives. Using this technique of oblique image acquisition, GSD varied in all images, but all features were photographed at least twice from no more than 5 m away, resulting in sub-millimeter resolution of all sampled areas. All sites were sampled during 9–13 September 2013.

We used PhotoScan v0.9.1 (Agisoft, St Petersburg, Russia) to derive point clouds and digital terrain models from imagery. GCPs were manually identified from the imagery, but otherwise the workflow (see Agisoft 2014) was mostly automated and involved (1) aligning images based on common features using feature recognition, (2) optimizing bundle adjustment to reduce root mean square error (RMSE) to less than a pixel, (3) creating the model surface using aerotriangulation, and (4) exporting the resulting 1-cm digital elevation model (DEM) and 1-mm GSD orthoimage. Camera calibration parameters were solved by the software by analyzing multiple views of the same surface acquired with varying camera orientations (Zhang 1999) and applied to the model. The software's ability to solve the camera calibration parameters of an off-

the-shelf digital camera liberates users from the requirement of using a calibrated mapping camera for high-precision photogrammetry. Surface model accuracy was assessed by measuring known objects in the images (ruler/DVDs).

Using the Surface Volume tool in ArcMap 10.0 (Esri, Redlands, CA), we calculated a range of soil loss from each headcut using the 1-cm DEMs from each site. We assumed that each headcut was once a gently sloping meadow/wetland similar to the area above the headcut (Fig. 2). The elevation of a point immediately upstream of the headcut became the horizontal reference plane below which volume was calculated. Because of the slight slope inherent in the riparian area, a non-sloped reference plane overestimates the fill volume in proportion to the slope of the riparian area. We attempted to detrend the slope from each DEM using a procedure detailed by Smart et al. (2002), but the irregular terrain of the riparian area confounded attempts to determine what degree of slope to detrend. Study sites were too small to utilize relatively coarse DEMs like the 10-m National Elevation Dataset. d’Oleire-Oltmanns et al. (2012) emphasized this point and used stereo glasses to digitize a “cap” along the gully headcut and sidewalls to

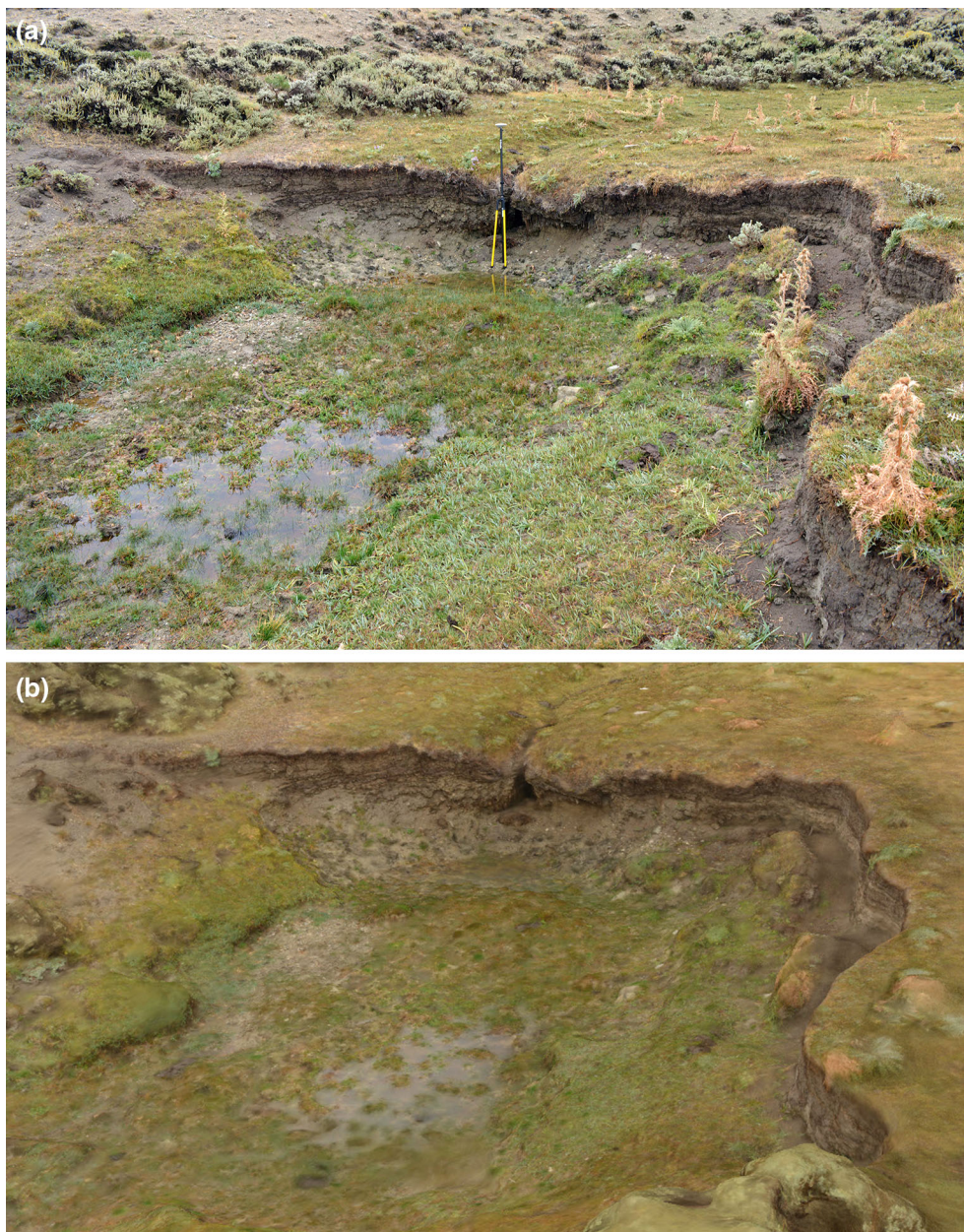


Fig. 2 **a** One of the most severe headcuts is located in Lower Coyote Gulch. The 2-m GPS tripod is placed against the headcut knickpoint for scale, showing that the meadow has been eroded a meter or more

below the upstream meadow surface. **b** Textured 3D terrain of the same site modeled from 415 images (see online supplementary material for 3D models) (color online)

act as the reference plane; however, the sidewalls of the headcuts we measured were irregular, making determination of where to digitize a 3D polyline unsatisfactorily subjective. Our alternative approach involved a second soil volume measurement using a reference elevation from a point on the *downstream* end of the headcut scour, where sediment aggradation raised the bed level above that at the base of the headcut. Because of channel slope, this calculation underestimates the headcut volume. Because the relationship between reference point elevation and headcut

volume is nonlinear (headcut volume increases exponentially with increased reference elevation), we could not calculate soil loss as the mean of the upper and lower reference plane soil loss values, or apply a constant offset to either, but instead we regard the interval as an estimated range of soil loss. This estimated range is narrow for sites with low slope and broader for sites with high slope, but in all cases encompasses with near certainty the true soil volume lost to erosion while maintaining an objective and repeatable measurement method. This approach would

likely not be very satisfactory for sites with very tall headcuts or very long scoured channels, but for the size of headcuts in this study, the method conveys a soil loss estimate with realistic precision. Channel thalweg length was measured from the derived orthoimage in ArcMap 10.0 and used to normalize soil volume to $\text{m}^3 \text{ m}^{-1}$ channel.

Results

Headcut Identification from Aerial Imagery

The 2008 survey captured three nested images at 1099 riparian locations (3297 images) along 15 named streams, of which 251 locations were of the Sweetwater River. From the remaining 848 locations, we identified 163 headcuts in seventy-three 1.4-cm GSD images (~9 % of the sample; Fig. 1). These headcuts were also visible in the 3.3-cm GSD imagery and were present in all surveyed drainages except the river channel itself. Because the 2008 imagery is discontinuous, this almost certainly undervalues the number of headcuts in the study area.

Three years after image acquisition, we visited eight of the identified headcuts and confirmed that all were indeed headcuts, some >1 m deep (Fig. 2a). The study area's vastness prevented additional ground confirmation, but ground observations revealed additional headcuts not noted from aerial imagery.

We did not identify any additional erosion features from 1-m GSD NAIP imagery acquired in 2012, and in fact were not able to recognize most of those headcuts identified from the 1.4-cm GSD imagery and subsequent ground observations; the resolution of NAIP, ~70× less than the 2008 imagery, was too coarse to discern such detail, though bare-soil patches sometimes hinted at headcut presence (Figs. 3, 4). Likewise, resolution of proprietary 30-cm GSD orthoimagery (ESRI 2014) was insufficient for headcut identification, and large headcuts were visible only when their locations and shapes were known a priori, and only when sun position advantageously created diagnostic shadows.

An important detail 30-cm or coarser resolution imagery does not show is the association of cattle trails and channel erosion (Fig. 3), and closely cropped or trampled vegetation. Approximately 90 % of the 1.4-cm GSD images showed herbivore trailing in the riparian zone that was not visible in the 1-m GSD NAIP imagery.

Terrain Model Creation and Volumetric Soil Loss Assessment from Ground-Based Imagery

Ground sampling required 42 h of field work over 5 days. Time spent photographing the sites was only 9 % of that,

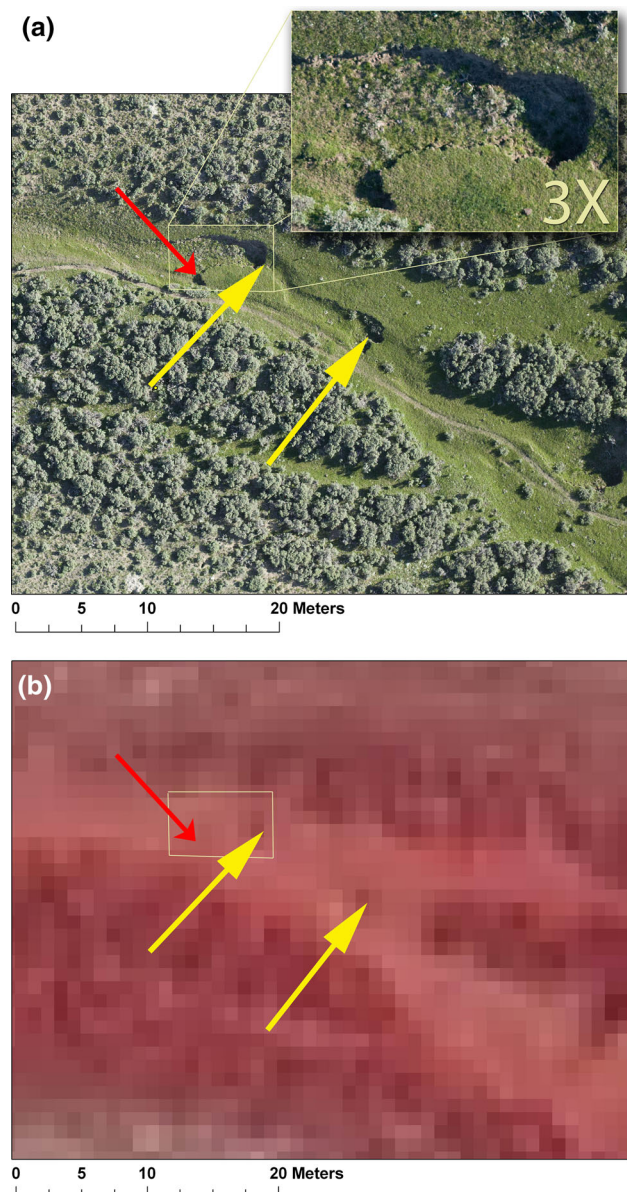


Fig. 3 Comparison of headcut feature detection using 1.4-cm (2008) and 1-m (2009 NAIP) resolution aerial imagery. Images are from the upper Sweetwater River subbasin south of the river. A 1.4-cm GSD image frame shows multiple headcuts (long, yellow arrowheads) in a stringer meadow (*top panel*). From right to left, note vegetation density above headcut compared to scoured channel below. Also note headcut following abandoned cattle trail (*short red arrowhead*). NAIP 1-m GSD 4-band imagery of the same area (*lower panel*) shows insufficient detail to confirm headcut presence (color online)

while collecting GCP data took 26 %. Simply driving to/from sites consumed 65 % of field time. On average, we spent 47 min at each site and 13 min photographing the headcut. We initially acquired 14-bit raw format imagery to take advantage of post-processing options, but found that the camera could not acquire images rapidly enough for efficient workflow. We therefore switched to low-compression 8-bit JPG images for all sites. Varying cloud cover caused varied

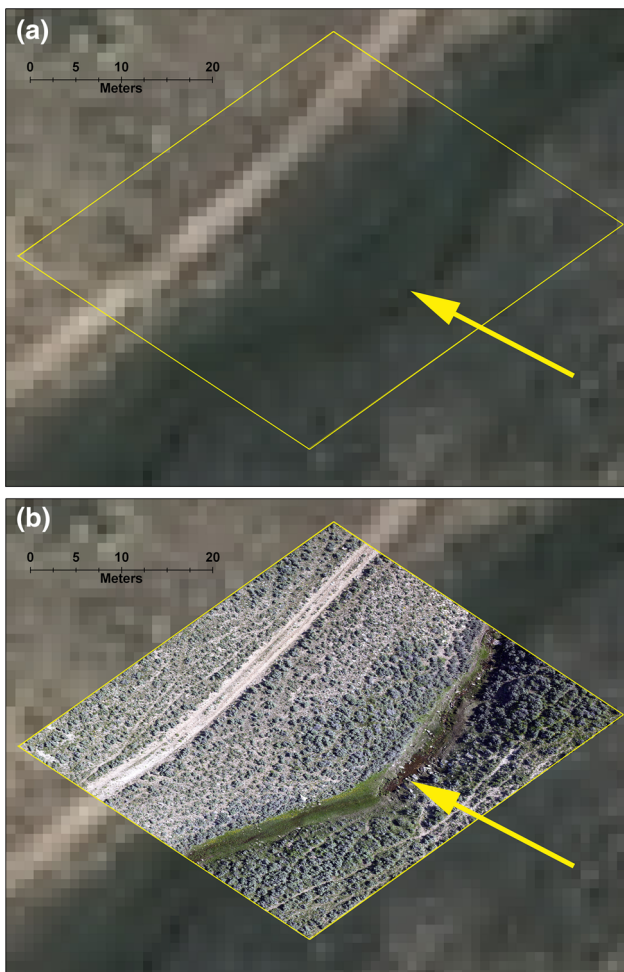


Fig. 4 Another comparison of headcut detection using 1-m and 1.4-cm resolution aerial imagery from the upper Sweetwater subbasin. The top panel shows 1-m GSD 2009 NAIP imagery, and the lower panel shows 1.4-cm GSD 2008 imagery (color online)

lighting, so camera parameters such as ISO, aperture, and shutter speed were optimized for each site to maximize image quality; however, once set, camera settings were unchanged for the entirety of acquisition at each site. Retaining constant lens element positions by prohibiting auto focus and aperture changes served to capture all images within a single camera calibration model, simplifying processing.

Surface models were created for 19 sites (e.g., Fig. 2b; *PDF models and site images available in online supplementary material*). Based on measurements of control objects, relative spatial accuracy ranged from 0.2 to 9 mm, with a mean accuracy across all sites of 2 mm (Table 2). Model RMSE for most sites was <0.5 pixel. Absolute spatial accuracy was lower; post-processed GPS data estimated that mean GCP accuracy was ± 22 cm. Site 1557, while showing severe erosion in the channel and crumbling banks, did not exhibit a defined headcut from which to

measure erosion volume. From 18 remaining sites, we estimate that 425–720 m³ of soil has been lost due to headcut erosion (51–86 three-axle dump truck loads), or on average 1.1–1.8 m³ m⁻¹ channel (Table 2). At some headcuts, there was no clear demarcation of the end of the downstream channel scour, and some qualitative judgment was required to determine where scour ended and sediment aggradation began. The headcut in lower Coyote Gulch was particularly large (Fig. 2), with an estimated soil loss of at least 133.2 m³, nearly 3× the minimum estimated soil loss of any other headcut, while the relatively minor headcut at Harris Slough appears to have lost a minimum of only 1.1 m³ of soil. More research is needed to understand such widely variable headcut retreat rates in drainages of close proximity.

Ground-sampled sites were not randomly chosen from the 163 identified headcuts. Those that we sampled with ground photography were among the most prominent, especially those along middle and lower Coyote Gulch. Because our sample purposefully included several unusually large headcuts, applying the mean soil loss from the 19 sampled headcuts in Table 2 to the remaining 144 headcuts identified from 2008 aerial imagery would likely overestimate soil loss for the 144-sample set. However, if we conservatively estimate that the remaining headcuts are on par with the *smallest* of the 19 headcuts from Table 2, then we might extrapolate those remaining 144 headcuts as having lost at least 3–5 m³ each, or a total of 432–720 m³. Summed with ground-sampled headcut soil loss, this would yield a conservative estimate of gully-erosion soil loss in the study area of 857–1440 m³. Much of the mineral soil is not completely lost from the system (Rieke-Zapp and Nichols 2011), but displaced downstream in a way that is less functional to the riparian system, damages the Sweetwater River fishery, and is indicative of lost water and carbon storage capacity.

Discussion

Headcut Monitoring

Headcuts indicate catastrophic degradation of riparian function, and the widespread presence of headcuts in the upper Sweetwater subbasin indicates widespread losses of water-storage capacity, reduced wildlife habitat quality, and degraded downstream fisheries. Temporal volumetric monitoring is essential for measuring progress toward the grazing-plan goal of increasing elevations of riparian water tables drained by large headcuts (BLM 2002, pg1), and for identifying the most active headcuts. Monitoring public land watersheds has not typically included headcut migration or volumetric analyses, nor has the imagery acquired been of

Table 3 Reported headcut volumetric erosion rates

$\text{m}^3 \text{ year}^{-1}$	Location	Land use	References
0.49	Spain	Rangeland	Marzolff et al. (2011)
1.95	Spain	Park	Campo-Bescos et al. (2013)
4.39	Spain	Cropland	Marzolff and Poesen (2009)
13.9	Spain	Cropland	Vandeckerckhove et al. (2003)
115	Arizona	Rangeland	Osborn and Simanton (1986)

sufficient resolution to detect most headcuts. Products such as headcut retreat rates and SfM-derived terrain models and soil volume measurements allow for rigorous, quantitative, and spatially based riparian monitoring. This study establishes a baseline for repeat surveys to determine headcut retreat, soil loss, and mitigation priorities. We calculated that the 18 meadows monitored in this study have each lost, on average, 24–40 m^3 of soil. Soil loss rate from gully erosion varies depending on environmental and geomorphological factors (Table 3; see Poesen et al. 2003 for a review of gully volumetric erosion rates). Compared to some regions, gully erosion soil loss in the Sweetwater subbasin is low, but is nevertheless ecologically significant because of the outsized importance of riparian areas in arid rangelands (BLM 1994).

We did not find conventional, 1-m GSD aerial imagery (NAIP) useful for identifying headcuts, much less modeling them, a finding consistent with Vandeckerckhove et al. (2003) who noted that conventional aerial photography resolution is insufficient for gully volumetric measurements. NAIP, and its similar forebearer, 1:40,000 (84 cm GSD¹) National Aerial Photography Program (NAPP) imagery represents the only public-domain statewide image source for Wyoming available for the last 30 years. Higher resolution aerial photography, on the order of 1:24,000 scale (50 cm GSD¹), is available for most of Wyoming in the 1970s and early 1980s and could potentially show sufficient detail for headcut modeling, according to successful monitoring efforts using similar-scale

aerial photography by Rieke-Zapp and Nichols (2011; 1:30,000 [63 cm GSD¹]), Vandekerckhove et al. (2003; 1:18,000–1:32,000 [38–67 cm GSD¹]), (Bouchnak et al. 2009; 1:25000 [30 cm GSD]), and Campo-Bescos et al. (2013; 1:13,500–1:20,000 [28–42 cm GSD¹]). However, these studies appear to have monitored large headcuts (>5 m) and such imagery would likely be less valuable for monitoring the much smaller headcuts in the Sweetwater subbasin, a finding underscored by the lack of observed headcut monitoring utility from 30-cm GSD imagery in this study (ESRI 2014). Martinez-Casasnovas et al. (2004) used 1:5000–1:7000 imagery (13–15 cm GSD¹), and Marzolff and Poesen (2009) used 1:6000–1:10,000 imagery (7–14 cm GSD) to successfully monitor 3–5-m-deep and wide headcuts in Spain, suggesting that monitoring headcuts in the Sweetwater subbasin, which are typically < 1 m deep, requires at least this image resolution. For Proper Functioning Condition Assessment of riparian areas in the western US, Prichard et al. (1996) recommended 1:40,000 imagery, but clarified that some applications require 1:3000 [6.3 cm¹ GSD] imagery. d’Oleire-Oltmanns et al. (2012) and Giménez et al. (2009) used 1.8- and 1.6-cm GSD aerial imagery, respectively, to model headcuts, and while the first study monitored headcuts much larger than those in the current study, the latter sampled headcuts of approximately the same size as those we sampled in the Sweetwater subbasin. In this context, the 1–2-cm GSD aerial imagery provided sufficient resolution for identifying and modeling headcuts of the size present in the Sweetwater subbasin. This is not to say that imagery in the 3–5 cm GSD range would be unusable, but we have confirmed evidence that 1–2-cm GSD imagery has high utility in this regard.

As an *ad hoc* test, we processed and modeled a series of the <2.5-cm GSD 2008 aerial images whose fields of view happened to overlap. The images were of two headcuts on a hummocked meadow along Strawberry Creek, and the resulting terrain model shows headcuts that, if we had used a GPS-IMU or GCPs, could be measured for headcut position, depth, and soil loss (Fig. 5)—thus illustrating the utility of very high-resolution aerial imagery. Given that 65 % of field time in this study was spent driving between study sites, aerial acquisition has the potential to greatly increase sampling efficiency and temporal resolution of monitoring imagery, a benefit that partially balances the inevitable loss of resolution relative to ground-based imagery.

With one exception, the study sites were ground-sampled (photographed) under overcast conditions, a rare phenomenon in arid central Wyoming that sidestepped problems from shadow-obscured areas. Giménez et al. (2009) discussed the obstacle to photogrammetry that shadows present, and concluded that techniques like SfM

¹ Estimated GSD based on scale and assumed scanning resolution of 21 $\mu\text{m pixel}^{-1}$. Aerial photographs can be scanned at a range of resolutions; however, for historical aerial photography there is a point at which increasing scan resolution does not improve the resolving power of the image and only creates an unnecessarily large digital file. Welch and Jordan (1996) recommend 17–33 $\mu\text{m pixel}^{-1}$, and Leberl et al. (2003) suggested 20 $\mu\text{m pixel}^{-1}$ scanning resolutions as optimizing detail and file size. The United States Geological Survey (USGS 2014b) provides maximum on-demand scanning of their historical photography archive at 14 $\mu\text{m pixel}^{-1}$. To provide a crosswalk between photography scale and digital image resolution when the resolution is not defined, we have included a calculated approximate GSD for historical imagery which assumes that historical aerial photography was scanned at 21 $\mu\text{m pixel}^{-1}$ (1200 dpi). This estimated GSD was not applied when cited studies listed imagery GSD.

Fig. 5 Textured terrain modeled from five stereo, 1.4-cm GSD nadir aerial images showing two headcuts along Strawberry Creek, 4 km north of the Sweetwater River (color online)



are unlikely to succeed in perpetually shadowed deep, narrow gullies. Marzolff and Poesen (2009) noted problems in SfM processing due to both shadows and overexposed bare-soil gully walls. While shadows and overexposed highlights are undesirable, capturing higher radiometric resolution in raw format (12- to 16-bits channel⁻¹), or bracketing exposures (± 3 f-stops) to capture the full contrast of a scene, as Cox and Booth (2008) detailed for vegetation monitoring, may allow full modeling of a gully's shadowed areas. Acquiring higher bit-depth imagery efficiently requires a camera capable of a high frame rate and a media card with a very fast write speed, otherwise excessive time is spent waiting on the camera to process and save images. Bracketing ground-based images is practical, but less so from aerial platforms. In the single instance of clear-sky acquisition we encountered, sufficient detail was captured in shadowed areas with 8-bit JPG images to create the terrain model and surface texture without overexposed highlights, but the sampled headcuts were also generally not deeply incised and narrow.

Only by recollecting images of the site and building a 3D model in the same coordinate space can temporal comparisons can be made. GPS error of ground control points, on the order of 22 cm, was disappointingly high and will complicate future efforts to capture the same terrain into the exact same coordinate space. We will henceforth strive to include permanent monuments at sites (rebar sunk down to below frost line, with top nearly level with the ground) or utilize higher accuracy GPS. We will also utilize coded circular targets in future projects. PhotoScan automatically recognizes coded circular targets and places tie markers on these locations automatically, greatly simplifying the image registration process.

The 3-year time lapse between image acquisition and ground-truth is problematic, and we cannot rule out the possibility that a false-positive headcut from the 2008 imagery may have become an actual headcut 3 years later. We regard this possibility as unlikely given the high resolving power of the 2008 imagery. In either event, a few such errors of commission among 163 identified headcuts would have little impact on our findings.

Conclusions

Our question was whether high-resolution imagery (0.2, 1.4, and 3.3 cm GSD) provided information not available from standard 1-m GSD imagery and whether that information could be used to enhance riparian ground monitoring. We conclude that using 30-cm and coarser resolution imagery—including the standard 1-m resolution imagery—to survey upper-elevation riparian systems is not effective and results in false negatives with respect to headcuts, channel scour, livestock trailing, and vehicle damage that are catastrophic channel erosion risks. Image resolution of 3.3 cm GSD or greater captured these indicators and was useful for assessing general conditions and for allowing an informed selection of locations for more intense ground-sampling efforts. Second, we conclude that the creation of SfM terrain models allows for fine-scale soil loss measurements and provides baseline positions for determination of gully erosion rates when appropriate ground control positioning and recording methods are employed.

We found abundant evidence that the meadows and wetlands of the upper Sweetwater subbasin are seriously

degraded. Widespread erosion has reduced or eliminated ecological services within the study area. We recommend using 1–3.3-cm GSD aerial imagery to screen for erosion features that are not noticeable in almost any commercial imagery product. We further recommend using 1–3.3-cm aerial or 1-mm GSD ground-based imagery to create terrain models using SfM to precisely quantify headcut retreat and erosion rates for determining management priorities.

Acknowledgments We thank Mike Londe, Tom Noble, and Drew Hurdle, BLM, for assistance with GPS data processing, camera and photogrammetric processing advice, and image processing assistance, respectively. Two anonymous reviewers provided constructive critiques. Mention of proprietary products does not constitute an endorsement or warranty by USDI, USDA, or the authors.

References

- Agisoft (2014) PhotoScan User Manual. St Petersburg, Russia. http://www.agisoft.ru/pdf/photoscan_pro_1_0_en.pdf Accessed 24 Jul 2014
- Antevs E (1952) Arroyo-cutting and filling. *J Geol* 60:375–385
- Avni Y (2005) Gully incision as a key factor in desertification in an arid environment, the Negev highlands, Israel. *Catena* 63:185–220
- Barnett TP, Pierce DW, Hidalgo HG, Bonfils C, Santer BD, Das T, Bala G, Wood A, Nozawa T, Mirin AA, Cayan DR, Dettinger MD (2008) Human-induced changes in the hydrology of the western United States. *Science* 319:1080–1083
- Belsky AJ, Matzke A, Uselman S (1999) Survey of livestock influences on stream and riparian ecosystems in the western United States. *J Soil Water Conserv* 54:419–431
- Beschta RL, Donahue DL, SellaSala DA, Rhodes JJ, Karr JR, O'Brien MH, Fleischner TL, Williams CD (2012) Adapting to climate change on western public lands: addressing the ecological effects of domestic, wild, and feral ungulates. *Environ Manage*. doi:10.1007/s00267-012-9964-9
- Bigelow CA, Bowman DC, Cassel DK (2004) Physical properties of three sand size classes amended with inorganic materials or sphagnum peat moss for putting green rootzones. *Crop Sci* 44:900–907
- BLM [Bureau of Land Management] (1994) Rangeland Reform'94. Draft environmental impact statement executive summary. US Department of the Interior, Bureau of Land Management & US Department of Agriculture, Forest Service https://ia601701.us.archive.org/27/items/rangelandreform9unit_0/rangelandreform9unit_0.pdf Accessed 27 Mar 2015
- BLM [Bureau of Land Management] (2002) Green mountain common allotment evaluation. US Department of the Interior, Bureau of Land Management, Lander
- Booth DT, Cox SE (2006) Very-large scale aerial photography for rangeland monitoring. *Geocarto Int* 21:27–34
- Booth DT, Cox SE, Likins JC (2015) Fenceline contrasts: grazing increases wetland surface roughness. *Wetl Ecol Manag* 23(2):183–194. doi:10.1007/s11273-014-9368-0
- BOR [Bureau of Reclamation] (2013) Literature synthesis on climate change implications for water and environmental resources, 3rd edn. US Department of the Interior, Denver, CO, USA. Technical Memorandum 86-68210-2013-06. <http://www.usbr.gov/climate/docs/ClimateChangeLiteratureSynthesis3.pdf> Accessed 11 Aug 2014
- Bouchnak H, Felfoul MS, Boussema MR, Snane MH (2009) Slope and rainfall effects on the volume of sediment yield by gully erosion in the Souar lithologic formation (Tunisia). *Catena* 78:170–177
- Brown JW, Schuster JL (1969) Effects of grazing on a hardland site in the southern High Plains. *J Range Manag* 22:418–423
- Bull WB (1997) Discontinuous ephemeral streams. *Geomorphology* 19:227–276
- Campo-Bescos MA, Flores-Cervantes JH, Bras RL, Casali J, Giraldez JV (2013) Evaluation of a gully headcut retreat model using multitemporal aerial photographs and digital elevation models. *J Geophys Res* 118:2159–2173
- Castelli RM, Chambers JC, Tausch RJ (2000) Soil-plant relations along a soil-water gradient in Great Basin riparian meadows. *Wetlands* 20:251–266
- Chimner RA, Cooper DJ (2003) Carbon dynamics of pristine and modified hydrologically modified fens in the southern Rocky Mountains. *Can J Bot* 81:477–491
- Corning RV (2002) Diminished Sweetwater River flows from the high cold desert region of Wyoming. 2002 Green Mountain Common Allotment Evaluation. US Department of the Interior Bureau of Land Management, Lander
- Cox SE, Booth DT (2008) Shadow attenuation with high dynamic range images. *Environ Monit Assess* 6:185–190
- d'Oleire-Oltmanns S, Marzolff I, Peter KD, Ries JB (2012) Unmanned aerial vehicle (UAV) for monitoring soil erosion in Morocco. *Remote Sensing* 4:3390–3416
- Dwir KA, Kauffman JB, Baham JE (2006) Plant species distribution in relation to water-table depth and soil redox potential in montane riparian meadows. *Wetlands* 26:131–146
- EPA [Environmental Protection Agency] (2014) Climate change indicators in the United States: Snowpack. <http://www.epa.gov/climatechange/science/indicators/snow-ice/snowpack.html> Accessed 6 Aug 2014
- ESRI (2014) World Imagery map service. http://www.arcgis.com/home/item.html?id=10df2279f9684e4a9f6a7f08febac2a9&_ga=1.100561558.981085741.1407863424 Accessed 11 Aug 2014
- FAA [Federal Aviation Administration] (2010) Airworthiness certification of aircraft and related products. Order 8130.2G. <http://www.faa.gov/documentLibrary/media/Order/8130.2G20.pdf> Accessed 07 Apr 2014
- Forsling CL (1931) US Forest Service Technical Bulletin No. 230. A study of the influence of herbaceous plant cover on surface runoff and soil erosion in relation to grazing on the Wasatch Plateau in Utah. US Department of Agriculture, Washington, D.C., USA
- Giménez R, Marzolff I, Campo MA, Seeger M, Ries JB, Casali J, Álvarez-Mozos J (2009) Accuracy of high-resolution photogrammetric measurements of gullies with contrasting morphology. *Earth Surf Proc Land* 34:1915–1916
- Greene RSB, Kinnell PIA, Wood JT (1994) Role of plant cover and stock trampling on runoff and soil erosion from semi-arid wooded rangelands. *Aust J Soil Res* 32:953–973
- Heede BH (1978) Designing gully control systems for eroding watersheds. *Environ Manage* 2:509–522
- Hudson BD (1994) Soil organic matter and available water capacity. *J Soil Water Conserv* 49:189–194
- Hunsaker CT, Neary DG (2012) Sediment loads and erosion in forest headwater streams of the Sierra Nevada, California. In: Proceedings of XXV IUGG General Assembly Workshop: Revisiting experimental catchment studies in forest hydrology, Melbourne, Australia. IAHS Publication, p 353
- Kauffman JB, Krueger WC (1984) Livestock impacts on riparian ecosystems and streamside management implications. *J Range Manag* 37:430–438
- Kauffman JB, Beschta RL, Otting N, Lytjen D (1997) An ecological perspective of riparian and stream restoration in the western United States. *Fisheries* 22:12–24

- Knowles N, Dettinger MD, Cayan DR (2006) Trends in snowfall versus rainfall in the western United States. *J Clim* 19:4545–4559
- Leberl F, Gruber M, Ponticelli M, Bernoegger S, Perko R (2003) The UltraCam large format aerial digital camera system. In: Proceedings of the American Society for Photogrammetry and Remote Sensing Annual Convention, Anchorage, AK, USA
- Ligon FK, Dietrich WE, Trust WJ (1995) Downstream ecological effects of dams. *Bioscience* 45:183–192
- Lusby GC (1970) Hydrologic and biotic effects of grazing versus nongrazing near Grand Junction, CO. Geological Survey Research Professional Paper 700-B. US Government Printing Office, Washington, DC, pp B232–B236
- Martinez-Casasnovas JA, Ramos MC, Poesen J (2004) Assessment of sidewall erosion in large gullies using multi-temporal DEMs and logistic regression analysis. *Geomorphology* 58:305–321
- Marzolff I, Poesen J (2009) The potential of 3D gully monitoring with GIS using high-resolution aerial photography and a digital photogrammetry system. *Geomorphology* 111:48–60
- Marzolff I, Poesen J, Ries JB (2011) Short to medium-term gully development: human activity and gully erosion variability in selected Spanish gully catchments. *Landf Anal* 17:111–116
- Mathews NA (2008) Technical Note 428. Aerial and close-range photogrammetric technology: Providing resource documentation, interpretation, and preservation. US Department of the Interior, Bureau of Land Management, Denver, CO, USA
- McCalla GR, Blackburn WH, Merrill LB (1984) Effects of livestock grazing on infiltration rates, Edwards Plateau of Texas. *J Range Manag* 37:265–269
- Mealo BA, Cox SE, Booth DT (2012) Postfire downy brome (*Bromus tectorum*) invasion at high elevation in Wyoming. *Invasive Plant Sci Manag* 5:427–435
- Meeuwig RO (1970) Infiltration and soil erosion as influenced by vegetation and soil in northern Utah. *J Range Manag* 23:185–188
- Miller RL, Fujii AE (2010) Plant community, primary productivity, and environmental conditions following wetland re-establishment in the Sacramento-San Joaquin Delta, California. *Wetla Ecol Manag* 18:1–16
- Mote PW, Hamlet AF, Clark MT, Lettenmaier DP (2005) Declining mountain snowpack in western North America. *Bull Am Meteorol Soc* 86:39–49
- Mudge JF, Baker LF, Edge CB, Houlahan JE (2012) Setting an optimal α that minimizes errors in null hypothesis significance tests. *PLoS One* 7(2):e32734. doi:[10.1371/journal.pone.0032734](https://doi.org/10.1371/journal.pone.0032734)
- Naiman RJ, Décamps H (1997) The ecology of interfaces: riparian zones. *Annu Rev Ecol Syst* 28:621–658
- Nayak A, Marks D, Chandler DG, Seyfried M (2010) Long-term snow, climate, and streamflow trends at the Reynolds Creek Experimental Watershed, Owyhee Mountains, Idaho, United States. *Water Resources Research* 46, W06519, doi:[10.1029/2008WR007525](https://doi.org/10.1029/2008WR007525)
- Nijhuis M (2014) When the snows fail. *Nat Geogr* 226(4):58–77
- Nusier OK (2004) Influence of peatmoss on hydraulic properties and strength of compacted soils. *Can J Soil Sci* 84:115–123
- Osborn HB, Simanton JR (1986) Gully migration on a southwest rangeland watershed. *J Range Manag* 39:558–561
- Parolo G, Rossi G (2008) Upward migration of vascular plants following a climate warming trend in the Alps. *Basic Appl Ecol* 9:100–107
- Pauchard A, Kueffer C, Dietz H, Daehler CC, Alexander J, Edwards PJ, Arévalo JR, Cavieres L, Guisan A, Haider S, Jakobs G, McDougall K, Millar CI, Naylor BJ, Parks CG, Rew LJ, Seipel T (2009) Ain't no mountain high enough: plant invasions reaching new elevations. *Front Ecol Environ* 7:479–486
- Pepin NC, Lundquist JD (2008) Temperature trends at high elevations: patterns across the globe. *Geophys Res Lett* 35:L14701. doi:[10.1029/2008GL034026](https://doi.org/10.1029/2008GL034026)
- Poesen J, Nachtergael J, Verstraten G, Valentin C (2003) Gully erosion and environmental change: importance and research needs. *Catena* 50:91–133
- Prichard D, Clemmer P, Gorges M, Meyer G, Shumac K (1996) BLM Technical Reference 1737–12. Using aerial photographs to assess proper functioning condition of riparian-wetland areas. US Department of the Interior, Denver
- Regonda SK, Rajagopalan B, Clark M, Pitlick J (2005) Seasonal cycle shifts in hydroclimatology over the western United States. *J Clim* 18:372–384
- Rieke-Zapp DH, Nichols MH (2011) Headcut retreat in a semiarid watershed in the southwestern United States since 1935. *Catena* 87:1–10
- Schumm SA, Hadley RF (1957) Arroyos and the semiarid cycle of erosion. *Am J Sci* 255:161–174
- Smart G, Duncan MJ, Walsh JM (2002) Relatively rough flow resistance equations. *J Hydraul Eng* 128:568–578
- Stavi I, Perevolotsky A, Avni Y (2010) Effects of gully formation and headcut retreat on primary production in an arid rangeland: natural desertification in action. *J Arid Environ* 74:221–228
- Stoddart LA, Smith AD, Box TW (1975) Effects of grazing upon infiltration. Range management, 3rd edn. McGraw-Hill Book Co, New York, pp 414–419
- Stromberg JC (2001) Restoration of riparian vegetation in the southwestern United States: importance of flow regimes and fluvial dynamism. *J Arid Environ* 49:17–34
- Tilt B, Braun Y, He D (2009) Social impacts of large dam projects: a comparison of international case studies and implications for best practice. *J Environ Manage* 90:S249–S257
- Trimble SW, Mendel AC (1995) The cow as a geomorphic agent—a critical review. *Geomorphology* 13:233–253
- Turner RM, Karpiscak MM (1980) United States Geological Survey Professional Paper 1132. Recent vegetation changes along the Colorado River between Glen Canyon Dam and Lake Mead, Arizona. US Government Printing Office, Washington, D.C., USA
- USDI [United States Department of the Interior] (2014) WY-050-11-01 Consolidated appeal decision on final grazing decision involving the arapahoe creek, antelope hills and alkali creek sheep allotments. Office of the Regional Solicitor, Denver
- USGAO [United States General Accounting Office] (1988) Public rangelands: Some riparian areas restored but widespread improvement will be slow. GAO/RCED-88-105. <http://babel.hathitrust.org/cgi/pt?id=uiug.30112000969292;view=1up;seq=1> Accessed 11 Aug 2014
- USGS [United States Geological Survey] (2014a) National Hydrography Dataset. <http://viewer.nationalmap.gov/viewer/nhd.html?p=nhd> Accessed 11 Aug 2014
- USGS [United States Geological Survey] (2014b) Aerial photo single frames. https://lta.cr.usgs.gov/Single_Frame_Records Accessed 22 Jul 2014
- Vandekerckhove L, Poesen J, Oostwoud Wijdenes D, Nachtergael J, Kosmas C, Roxo MJ, De Figueiredo T (2000) Thresholds for gully initiation and sedimentation in Mediterranean Europe. *Earth Surf Proc Land* 25:1201–1220
- Vandekerckhove L, Poesen J, Govers G (2003) Medium-term gully headcut retreat rates in SE Spain determined from aerial photographs and ground measurements. *Catena* 50:329–352
- Welch R, Jordan TR (1996) Using scanned air photographs. In: Morain S, Baros SL (eds) Raster imagery in geographic information systems. OnWord Press, Santa Fe, pp 55–69
- Westoby MJ, Brasington J, Glasser NF, Hambrey MJ, Reynolds JM (2012) ‘Structure-from-Motion’ photogrammetry: a low-cost, effective tool for geoscience applications. *Geomorphology* 179:300–314
- Zald HSJ (2009) Extent and spatial patterns of grass bald land cover change (1948–2000), Oregon Coast Range, USA. *Plant Ecol* 201:517–529

Zhang Z (1999) Flexible camera calibration by viewing a plane from unknown orientations. In: Proceedings of the seventh IEEE international conference Vol 1

Zheng F, He X, Gao X, Zhang C, Tang K (2005) Effects of erosion patterns on nutrient loss following deforestation on the Loess Plateau of China. *Agric Ecosyst Environ* 108:85–97